ACCOUNTS
of chemical research

Liquid Water: From Symmetry Distortions to Diffusive Motion

NOAM AGMON*

The Fritz Haber Research Center, Institute of Chemistry, The Hebrew University of Jerusalem, Jerusalem 91904, Israel

RECEIVED ON MARCH 8, 2011

CONSPECTUS

Water deviates from tetrahedral symmetry on different scales, creating "defects" that are important for its dynamics. In this Account, I trace the manifestations of these distortions from the isolated molecule through gas-phase clusters to the liquid phase.

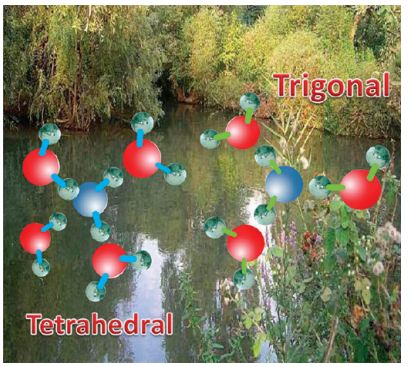

Unlike the common depiction, an isolated water molecule has a nonsymmetric charge distribution: although its positive charge is localized at the hydrogens, the negative charge is smeared between the lone-pair sites. This creates a "negativity track" along which a positive charge may slide. Consequently, the most facile motion within the water dimer is a reorientation of the hydrogen-bond (HB) accepting molecule (known as an "acceptor switch"), such that the donor hydrogen switches from one lone pair to the other.

Liquid water exhibits asymmetry between donor and acceptor HBs. Molecular dynamics simulations show that the water oxygens accepting HBs from the central molecule are spatially localized, whereas water hydrogens donating HBs to it are distributed along the negativity track. This asymmetry is manifested in a wider acceptor- versus donor-HB distribution. There is a higher probability for a water molecule to accept one (trigonal symmetry) or three HBs than to donate one or three HBs. A simple model can explain semiquantitatively how these distributions evolve by distorting perfectly tetrahedral water. Just two reactions are required: the dissociation of a HB between a double-donor donating to a double-acceptor, $D_2\cdot\cdot A_2$, followed by a switching reaction in which a HB donor rotates its hydrogen between two double-acceptor molecules.

The preponderance of $D_2\cdot\cdot A_2$ dissociation events is in line with HB "anticooperativity", whereas positive cooperativity is exhibited by conditional HB distributions: a molecule with more acceptor bonds tends to have more donor bonds and vice versa. Quantum mechanically, such an effect arises from intermolecular charge transfer, but it is observed even for fixed-charge water models. Possibly, in the liquid state this is partly a collective effect, for example, a more ordered hydration shell that enhances the probability for both acceptor and donor HBs.

The activation energy for liquid water self-diffusion is considerably larger than its HB strength, pointing to the involvement of collective dynamics. The remarkable agreement between the temperature dependence of the water self-diffusion coefficient and its Debye relaxation time suggests that both share the same mechanism, likely consisting of coupled rotation and translation with collective rearrangement of the environment.

The auto-correlation function of a hydrogen-bonded water molecule pair is depicted quantitatively by the solution of the diffusion equation for reversible geminate recombination, up to long times where the ubiquitous $t^{-3/2}$ power law prevails. From the model, one obtains the HB dissociation and formation rate coefficients and their temperature dependence. Both have a similar activation enthalpy, suggesting rapid formation of HBs with alternate partners, perhaps by the HB switching reaction involving the trigonal site.

A detailed picture of how small fluctuations evolve into large-scale molecular motions in water remains elusive. Nonetheless, our results demonstrate how the plasticity of water can be traced to its asymmetric charge distribution, with duality between tetrahedral and trigonal ligation states.

Published on the Web 10/06/2011 www.pubs.acs.org/accounts
10.1021/ar200076s

1. Introduction

Ice exhibits a nearly perfect tetrahedral symmetry around each water molecule.[1,2] Liquid water deviates from tetrahedral symmetry on many distance and time scales. This brings water to life, allowing for facile dynamics so that its molecular mobility is similar in magnitude to that of nonassociated liquids.[3−7] Water dynamics, in turn, brings life to Earth.[8] Thus the question of how local defects in the tetrahedral structure of water are amplified with time and distance until molecular motion becomes feasible is an interesting, yet complex problem. The present exposition is an effort to connect the deviations from symmetry observed on local distance scales and short times with hydrogen-bond (HB) distributions and molecular diffusion, which spans larger distances and occurs on slower time scales.

The literature on water structure and dynamics is vast as an ocean, with frequent whirlpools of contradictions and disputes. Here, results from Jerusalem[9−14] will be discussed in the broader perspective of existing experimental and simulation work. The reader will nevertheless realize that despite the huge effort devoted to water dynamics, a detailed molecular picture of how small fluctuations evolve into large scale molecular motions still remains elusive.

2. Deviations from Tetrahedrality

To an extent, the widespread perception of water as tetrahedral may be attributed to the valence shell electron pair repulsion (VSEPR) model.[15,16] Of the six valence electrons of the oxygen atom, two are involved in the two σ orbitals of the covalent OH bonds. The remaining four reside in two "lone pair" (LP) orbitals. According to VSEPR, these four orbitals arrange in the most spherically symmetric way, occupying alternate corners of a cube (Figure 1). Subsequently, the LPs "push" the hydrogens together, so that the HOH angle, 104.5°, is slightly below the tetrahedral angle of 109.5°. The widespread dogma perceiving "the excess negative charge ... around the oxygen atom as organized primarily in two lobes, or LP orbitals",[17] is depicted graphically by LPs sticking out like "rabbit's ears" (Figure 2). Unfortunately, this view is not in accord with either theory or experiment.[18] The distribution of positive and negative charge around a water molecule is nonsymmetric, and this gives rise to HB "defects" that facilitate water dynamics.

2.1. On the Negativity Track. Quantum calculations show that while the positive charge in a water molecule is localized near the hydrogen atoms, the negative charge is smeared out on the oxygen side between the LPs.[19] This

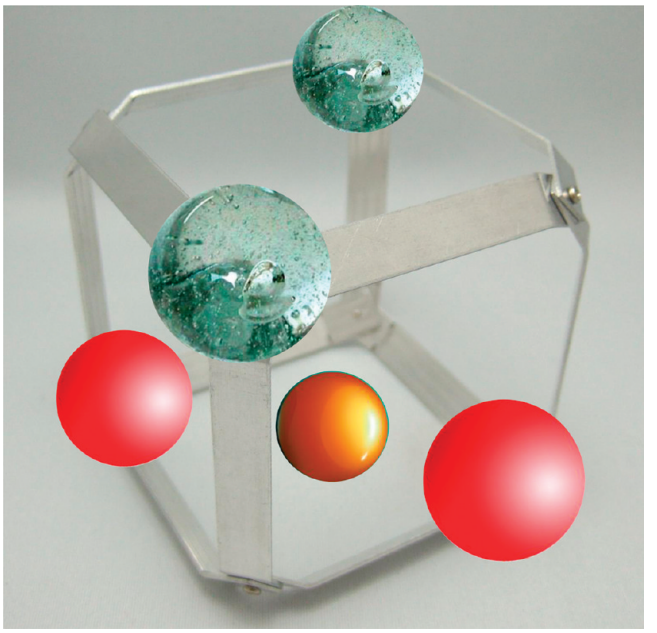

FIGURE 1. The vertices of a tetrahedron depicted as four alternating corners of a cube. With the oxygen atom in the center (not shown), the two hydrogen atoms (crystal balls) and two LPs (red balls) of a tetrahedral water molecule occupy the indicated sites. In reality, the negative electron density extends between the LPs to the orange trigonal site.

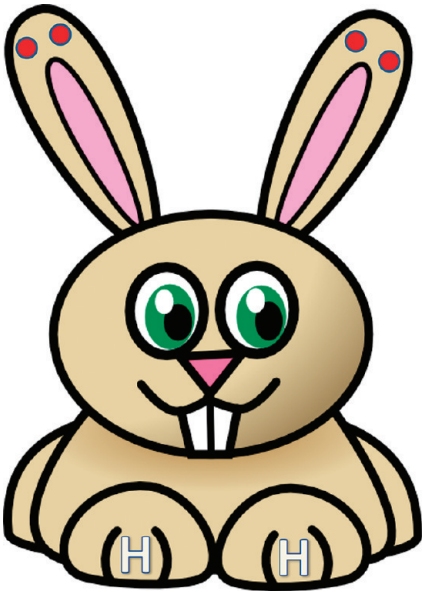

FIGURE 2. A popular visualization of the LPs of a water molecule (red circles) as rabbit's ears sticking out into space (the head then depicts the oxygen atom and the two front feet depict the hydrogen atoms).

"negativity track" is conceivably a superposition of electron density in the LP sites and the "trigonal site", located along the bisector of the HOH angle (orange ball in Figure 1). Analogous behavior is exhibited by the "electron localization function" (ELF),[20] see Figure 3.

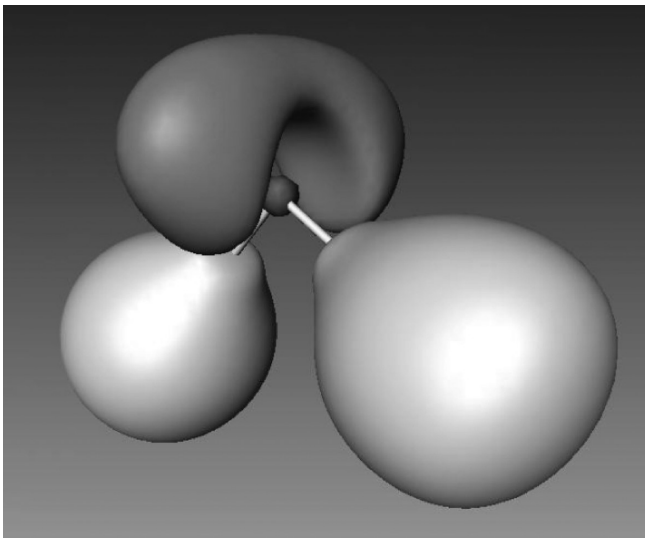

FIGURE 3. ELF depiction of the "negativity track" for a single water molecule, see also Figures 8 and 9 in ref 20 and Figure 9a in ref 16. The oxygen core connects by sticks to the hydrogen localization basins with the LP density on top. Courtesy of Ronald J. Gillespie.

The negativity track facilitates the motion of a positively charged ligand between the two LP sites. This is demonstrated by high-resolution spectroscopic studies of water clusters.[21] In the water dimer, the donor hydrogen forms a hydrogen bond (HB) with one LP on the acceptor oxygen (Figure 4A). Vibrational–rotational tunneling spectra indicate that the most facile molecular motion (with a barrier of only 157 cm^{-1}) is "acceptor switching" between its two LP sites.[21] In the cyclic trimer, an apparently barrierless motion flips the unbound hydrogen from one side of the trioxygen plane to the other (Figure 4B). Why are acceptor flips so facile? If the LP orbitals were localized at two corners of a tetrahedron, an acceptor flip would have encountered a similar barrier to that of a donor flip, which is actually the motion with the highest barrier for the dimer (394 cm^{-1}, see Figure 4 in ref 21). Acceptor switching must therefore take advantage of the "negativity track": the donor hydrogen can follow this track from one LP site to the other without ever dissociating its HB.

In some situations the secondary "trigonal site" may actually become dominant. A nice example is cation solvation. A recent experimental study demonstrated the insensitivity of dielectric relaxation (DR) spectroscopy toward anionic hydration and of fs-IR spectroscopy toward cationic hydration.[22] This was interpreted as evidence that a first-shell water molecule points its O–H toward the anion, whereas its dipole moment is directed away from the cation (Figure 5). The interaction with the

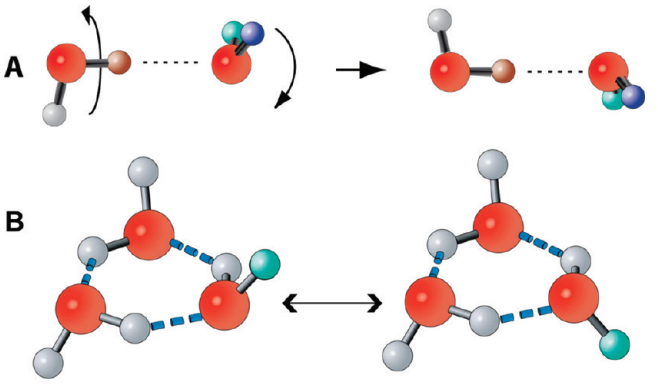

FIGURE 4. The low barrier acceptor flip motions in the water dimer (A) and trimer (B) are conjectured here to proceed with the donor hydrogen sliding along the "negativity track", see also Figures 4 and 5 of ref 21. Courtesy of Frank N. Keutsch and Richard J. Saykally.

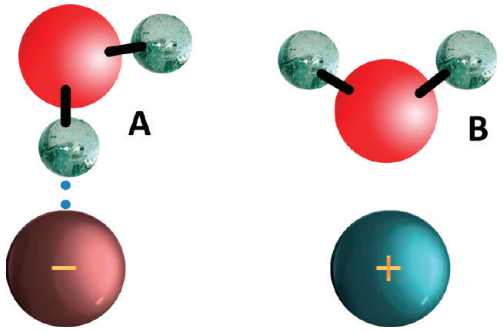

FIGURE 5. Different hydration water orientations are deduced to occur in the first solvation shell on anions and cations: (A) an anion orients the OH bond toward it, whereas (B) a cation orients the water dipole moment vector away from it. See Figure 3 of ref 22.

cation is thus directed to the trigonal rather than the tetrahedral site.

The most extreme example is provided by the hydrated proton, which forms a truly covalent bond through the trigonal site. The ensuing hydronium, H_3O^+, has three equivalent OH bonds. Being isoelectronic with ammonia, NH_3, it too adopts a trigonal pyramid geometry (Figure 6). Thus the geometry has changed here all the way from tetrahedral to trigonal.

2.2. Solvation Shells. Liquid water exhibits local tetrahedral symmetry from which deviations occur already in the first solvation shell. The local tetrahedral order is evident from the oxygen–oxygen radial distribution function (RDF), $g(r)$, which describes the density of oxygen atoms as a function of distance, r, from a reference water molecule. The X-ray scattering results[23] in Figure 7 show a series of peaks for consecutive solvation layers.

One can deduce the location of the maxima and minima from a simple tetrahedral model.[9] In tetrahedral symmetry,

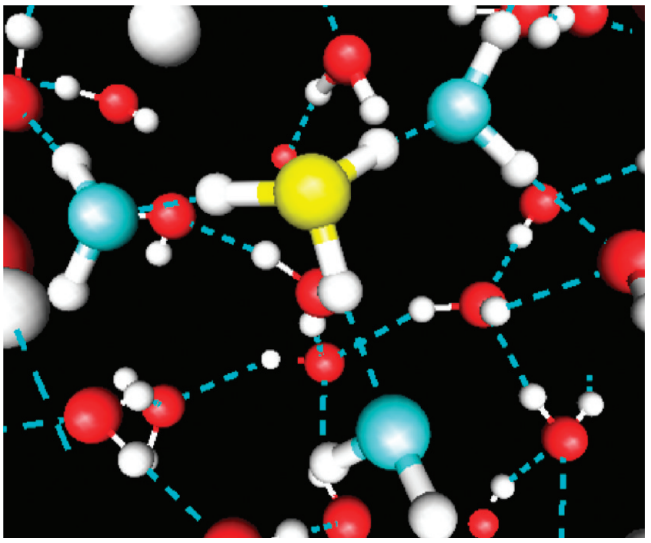

FIGURE 6. The hydronium ion, H_3O^+, as visualized from a molecular simulation.[11] Hydrogens are white and oxygens red, except for the hydronium oxygen (in yellow) and its first shell ligands (in cyan). HBs shown by dashed lines.

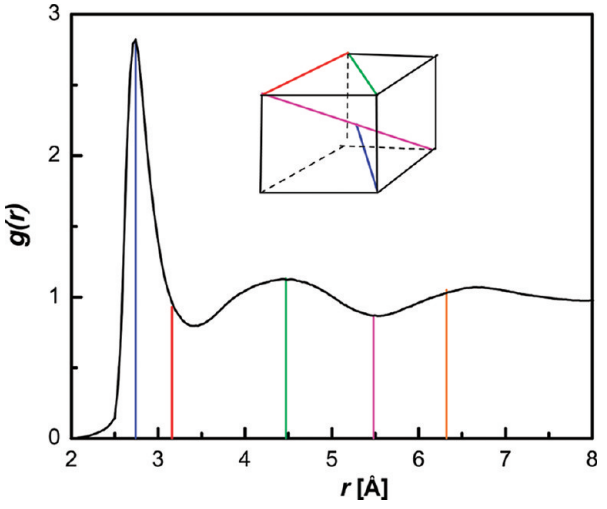

FIGURE 7. Predicted distances of maximal and minimal densities from a tetrahedral model for the oxygen–oxygen RDF of liquid water, taken from X-ray diffraction data at 27 °C (black line).[23] Redrawn after Figure 2 of ref 9. With the first peak at $r \equiv 2.74$ Å, the model predicts subsequent minima/maxima at $2r/3^{1/2}$, $(8/3)^{1/2}r$, $2r$, and $4r/3^{1/2}$ (vertical lines with colors corresponding to distances within the cube in the inset). Note that the first minimum occurs at a somewhat larger distance than predicted, likely due to a small interstitial peak at that location. Experimental data courtesy of Teresa Head-Gordon.

with the reference water molecule at the center of a cube and its first-shell neighbors at four alternating corners (cf. Figure 1), the distance to the first solvation layer is half the main diagonal, to the second is the face diagonal, and to the third is twice the side of the cube. With the cube dimensions determined from the first peak at 2.74 Å, the

FIGURE 8. Spatial density function of oxygen (red) and hydrogen (white) in the first solvation shell of a (ball-and-stick rendered) water molecule at room temperature, calculated using quantum simulations with the ab initio based polarizable TTM2.1-F water model (see Figure 8 of ref 26 for details). Courtesy of Francesco Paesani and Gregory A. Voth.

other two distances are predicted in agreement with the subsequent two maxima in Figure 7. Tetrahedral symmetry predicts also minimal densities at distances equal to the side of the cube and its main diagonal. However, a peak assigned to the third nearest neighbor in the hexagonal boat structure of ice I_h is already absent in liquid water.[24] Thus while the local water structure is tetrahedral, two adjacent water tetrahedra do not maintain the ideal orientation as in ice.

Deviations from tetrahedrality in the first solvation shell are evident from the spatial distribution function (SDF), depicting the angular distribution around a central water molecule, as obtained from molecular dynamics (MD) simulations.[25,26] As Figure 8 shows, the oxygens accepting HBs from the two hydrogen atoms of the central water molecule occupy two narrow caps above these hydrogens, whereas the hydrogens donating HBs to the central oxygen are distributed along the "negativity track". The loss of tetrahedral order with increasing temperature is attributed, accordingly, to water hydrogens that "are no longer located preferentially toward the lone pairs of the central molecule".[27]

2.3. Counting Hydrogen Bonds. The asymmetry between the donor and acceptor properties of water molecules is manifested in the HB distributions for liquid water, as obtained from classical MD simulations (even though

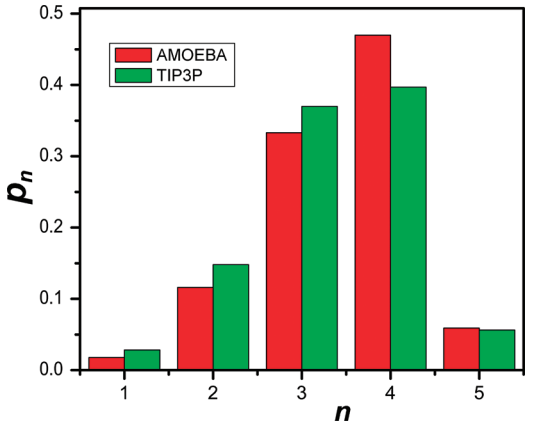

FIGURE 9. Probability, p_n, for a water molecule to have n HBs, calculated from classical trajectories at 300 K. The comparison of AMOEBA with flexible TIP3P water models shows that the distribution does not depend strongly on the model. Data from Table 1 of ref 12.

customary water models do not include the negativity track explicitly). Calculating them requires, of course, a working definition of a HB. Whether geometric, energetic, or topological in nature, it will always possess some degree of arbitrariness. A comparison of various definitions utilized in the literature can be found in ref 28, with more recent "topological" definitions in refs 29 and 30. For a qualitative understanding, the differences between most reasonable definitions is not large. We have utilized the geometric "R–β" definition,[31] where R and β are the maximally allowed values of the O–O distance and HOO angle (i.e., the angle between the O–H and O–O vectors for an O–H···O HB), respectively. R is approximately the first minimum in $g(r)$, ca. 3.5 Å at ambient conditions, whereas $\beta \leq 30°$. Calculations reported herein[12,13] are mostly from classical trajectories using the polarizable AMOEBA water model,[37] in a box containing 500 water molecules at a density of 0.996 g/cm^3.

Commonly calculated is p_n, the probability for a water molecule to engage in n HBs,[27,32–36] such as shown in Figure 9. Liquid water deviates from tetrahedrality, for which $p_4 = 1$ and $p_{n\neq 4} = 0$. The nontetrahedral configurations with $n = 3$ and 5 are considered as "defects" that catalyze reorientation and diffusion of water molecules.[3–7] A fundamental question is what is the nature of these defects? It was previously assumed[3–6] that $n = 5$ corresponds predominantly to a bifurcated hydrogen bond (BHB):[38,39] "A consequence of a fifth bonded molecule in the first coordination shell is that a proton is shared by two different oxygen atoms".[3] This BHB, depicted schematically in Figure 10A, "is actually a *local minimum* on the energy hypersurface".[3] "The emergence of more perfect tetrahedral network with

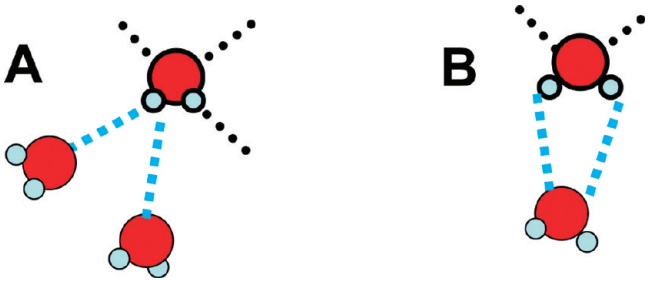

FIGURE 10. Two types of BHBs:[39] (A) bifurcated hydrogen (the "standard" BHB) and (B) bifurcated oxygen. The latter "refers specifically to the case where both donated protons are from the same donor atom"[39] and not to a case where "one of the two LPs accepts protons from two different molecules".[4]

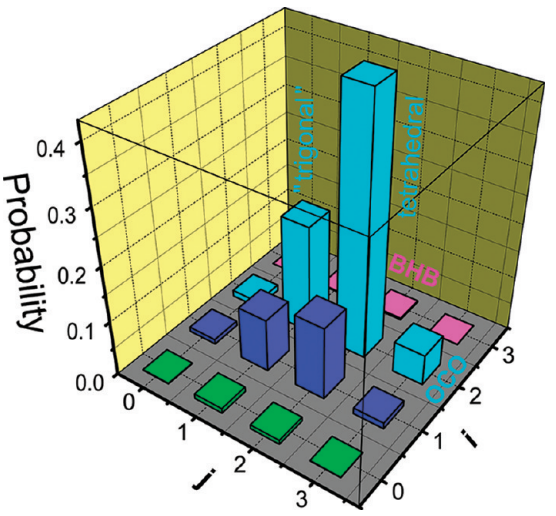

FIGURE 11. Joint probability, $p_{i,j}$, for a water molecule to have i donor HBs and j acceptor HBs, calculated from classical AMOEBA trajectories at 300 K. Data from Table 1 of ref 12.

decreasing density" is because "the fraction of water molecules with more than four HBs, i.e. with at least one BHB, decreases drastically".[6]

These statements are incorrect, as can be shown by counting *separately* donor and acceptor HBs. Most detailed is the joint acceptor–donor distribution, $p_{i,j}$, namely, the probability that a water molecule donates i HBs and accepts j HBs. It has been calculated in some recent work,[2,25,40] though rarely including the $i = 3$ and $j = 3$ states.[2] Our AMOEBA results[12] are shown in Figure 11: The highest peak, $p_{2,2}$, corresponds to tetrahedral symmetry, whereas the second highest, $p_{2,1}$, depicts trigonal symmetry (with a single acceptor bond). The third highest value is $p_{1,2}$. These three peaks comprise about 80% of all HBed configurations.

One can now identify the five-neighbor defect: the row with $i = 3$ corresponds to a BHB, whereas the column with

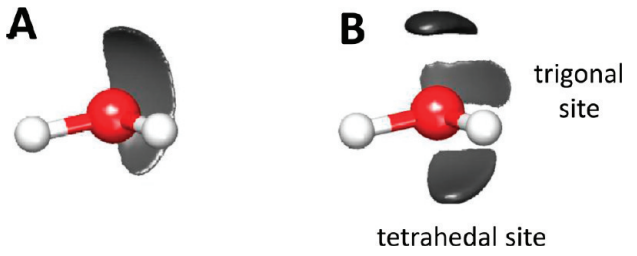

FIGURE 12. Acceptor-bond SDF for a water molecule with (A) one and (B) three acceptor bonds. The gray caps denote the three-dimensional densities of donating hydrogens in the first hydration shell of the central water molecule. From a TIP4P/2005 simulation at 298 K,[30] courtesy of Richard H. Henchman.

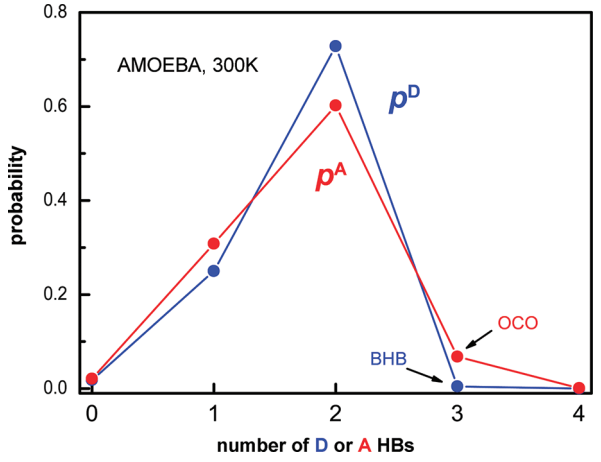

FIGURE 13. The probability for a water molecule (in AMOEBA simulations at 300 K) to engage in a given number of donor (D) or acceptor (A) bonds. Data tabulated in the Supporting Information. Lines are to guide the eye.

$j = 3$ corresponds to an over-coordinated oxygen (OCO), which accepts three HBs. Clearly, OCOs dominate over BHBs. The partial SDF (as opposed to the full SDF in Figure 8) for acceptor HBs of water molecules accepting either one or three HBs (Figure 12) demonstrates that the third OCO ligand binds through the trigonal site, rather than to a LP that "accepts protons from two different molecules".[4]

The asymmetry between HB donor and acceptor is seen even more clearly in Figure 13, which depicts the (unconditional) donor and acceptor distributions, $p_i^D \equiv \sum_j p_{i,j}$ and $p_j^A \equiv \sum_i p_{i,j}$, for states D_i (i donor bonds) and A_j (j acceptor bonds), respectively. These two distributions, from AMOEBA trajectories at four temperatures,[12] are tabulated in the Supporting Information. The probability for an OCO (p_3^A) is nearly a factor 14 larger than that for a BHB (p_3^D), in agreement with the assessment that BHBs are transition states rather than stable intermediates (cf. Figure 13 in ref 30). Indeed, stable BHBs were reported for crystals, intramolecular HBs, and stronger proton donors than water.[41] Apparently, in liquid water the HBs are too weak and the disorder too large for sustaining stable BHBs.

2.4. Modeling Donor and Acceptor Distributions. Figure 13 shows that the acceptor distribution is *wider* than the donor distribution. This observation is the basis for a model for generating the observed distributions from "ideal" tetrahedral symmetry. First, we note that with good approximation

$$p_1^A = p_1^D + (p_2^D - p_2^A)/2 \tag{1a}$$

$$p_3^A = p_3^D + (p_2^D - p_2^A)/2 \tag{1b}$$

Indeed, this formula gives $p_1^A = 0.313$ vs the simulation value of 0.308, and $p_3^A = 0.067$ vs 0.068.

Suppose that "initially" the two distributions were identical, $p_j^D = p_j^A$ and then p_j^A widened (without changing p_j^D). Denoting its variation by $\Delta p_j^A \equiv p_j^A - p_j^D$, eq 1 implies that $\Delta p_3^A = -\Delta p_2^A/2 = \Delta p_1^A$. This corresponds to conversion of two double-acceptor (DA) molecules into one single- and one triple-acceptor (OCO):

$$A_2 + A_2 \rightarrow A_1 + A_3 \tag{2}$$

a HB analog of the water disproportionation reaction, $2H_2O \rightarrow H_3O^+ + OH^-$. It likely occurs by a third water molecule switching its donor hydrogen from one A_2 to the other,[30] conceivably via the "jump mechanism" of water reorientation.[42,43]

This switching reaction is at equilibrium with an equilibrium coefficient

$$K_{sw} \equiv p_1^A p_3^A/(p_2^A)^2 \tag{3}$$

Rewriting eq 1 as $p_1^A + p_2^A + p_3^A = p_1^D + p_2^D + p_3^D$ and $p_1^A - p_3^A = p_1^D - p_3^D \equiv \alpha$ and inserting into eq 3, one obtains a quadratic equation for p_j^A in terms of the p_i^D. For example, its solution for p_1^A is

$$2(1 - 4K_{sw})p_1^A = \alpha - \beta \pm [\alpha^2 + \beta(p_2^D + 2p_3^D)]^{1/2} \tag{4}$$

where $\beta \equiv 4K_{sw}(p_2^D + 2p_1^D)$.

It remains to consider how the p_i^D might be generated from the perfectly tetrahedral state, $p_2^D = p_2^A = 1$. The simplest scenario is one in which DAs and DDs (double donors) dissociate in pairs

$$A_2 + D_2 \rightarrow A_1 + D_1 \tag{5}$$

Although written as a bimolecular reaction, the reactants involve a DD donating a HB to a DA, $D_2 \cdots A_2$ (the dotted

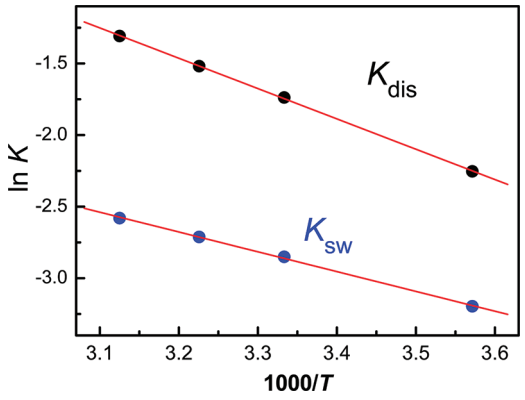

FIGURE 14. A van't Hoff plot for the simulated equilibrium constants (circles) of the HB dissociation and switching reactions, eq 2 and eq 5. Data from AMOEBA donor and acceptor distributions in the Supporting Information, calculated from the $p_{i,j}$ of ref 12.

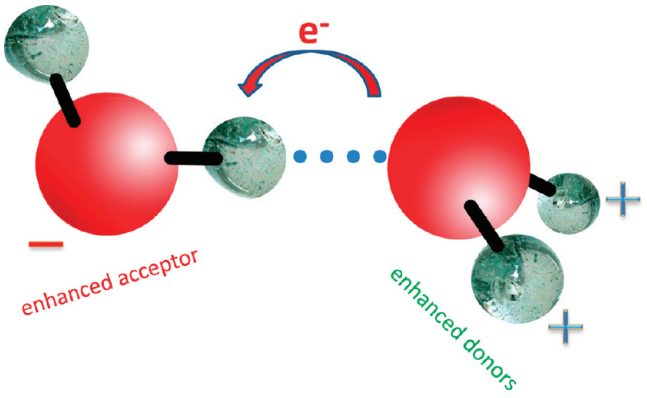

FIGURE 15. Electron density migration in the water dimer.[44]

line denotes here a directional HB). Starting from $(i,j) = (2,2)$, this generates the states (2,1), (1,2), and (1,1), but not states with $i = 0, j = 0$ or $i = 3$ (BHB), ca. 4% of the population. In liquid water, this dissociation reaction is at equilibrium with

$$K_{dis} \equiv p_1^A p_1^D / (p_2^D p_2^A) \qquad (6)$$

Figure 14 shows a van't Hoff plot for the temperature dependence of K_{sw} and K_{dis}. The corresponding reaction enthalpies are $\Delta H_{dis} \equiv -0.5R\ \mathrm{d}(\ln K_{dis})/\mathrm{d}(1/T) = 8.8$ kJ/mol and, similarly, $\Delta H_{sw} = 5.8$ kJ/mol (the reactions are written for 2 mols; hence the division by 2). ΔH_{dis} depicts the HB strength for this water model, whereas $\Delta H_{dis} - \Delta H_{sw} = 3$ kJ/mol is the strength of a HB to the trigonal acceptor site of an OCO, that is, for dissociating $D_2\cdots A_3$ pairs. Because $\Delta H_{dis} > \Delta H_{sw}$, the main effect of raising the temperature is the dissociation of additional $D_2\cdots A_2$ pairs, while the OCO probability hardly changes.

2.5. Short-Range Cooperativity, Long-Range Correlations. Quantum chemistry suggests that cooperativity occurs on the level of a water dimer, due to $n \rightarrow \sigma^*$ charge transfer (CT) from a LP to the OH antibonding σ orbital.[44] The hydrogens of the HB accepting water become more positive, while the oxygen of the HB donating water becomes more negative (Figure 15). The dimer is thus a better HB donor and a better acceptor (and has a larger dipole moment) than the monomer. Addition of a third water molecule in the same orientation, $OH_2\cdots OH_2\cdots OH_2$, strengthens this HB (three-body cooperativity), whereas for the opposing orientation, $H_2O\cdots HOH\cdots OH_2$, this HB weakens (anticooperativity).[45,46] As a result, small water clusters tend to form linear or cyclic chains. Indeed, a quantum chemistry study of larger clusters (up to 22 water molecules) found that "all two-coordinated molecules are single donors".[47] Ab initio simulations found the air–water interface enriched in doubly coordinated water molecules.[48] These observations may be attributed to CT cooperativity.

Cooperativity is manifested in the HB lengths of small water clusters.[21] The O–O distance in the water dimer is 2.95 Å, dropping to 2.85 Å in the cyclic trimer. This occurs despite the ring strain in the three-membered ring, which is therefore overcome by a sizeable three-body term. In the cyclic tetramer, the O–O distance shrinks further to 2.79 Å, whereas in the cyclic pentamer, it drops to 2.72 Å. This may be due to "the effect of many-body forces" (Figure 8 in ref 21). However, given that four-body terms are already quite small,[45] it may alternately result from ring-strain relief: making HBs more linear should increase the magnitude of both two- and three-body terms.

Interestingly, the HB distributions from liquid water simulations also show cooperative-like behavior. To see that, we define *conditional* HB distributions.[12] For example, the conditional donor distribution is obtained by dividing $p_{i,j}$ by p_j^A:

$$p^D(i|j) \equiv \frac{p_{i,j}}{\sum_i p_{i,j}} \qquad (7)$$

For independent donor and acceptor bonds $p^D(i|j)$ has no j dependence. Figure 16 shows that the two bonds *are not* independent: large j tends to shift the distribution to larger i. This appears as positive cooperativity, where acceptor bonds enhance the probability of having donor bonds.

For reference, the figure shows similar results from a flexible TIP3P simulation.[12] The effect is larger for the polarizable AMOEBA model, which may be due to CT cooperativity. However, the fact that it exists at all for the fixed-charge TIP3P potential indicates that there are additional mechanisms for deviation from independence, such as collective motions and solvent effects. A more ordered

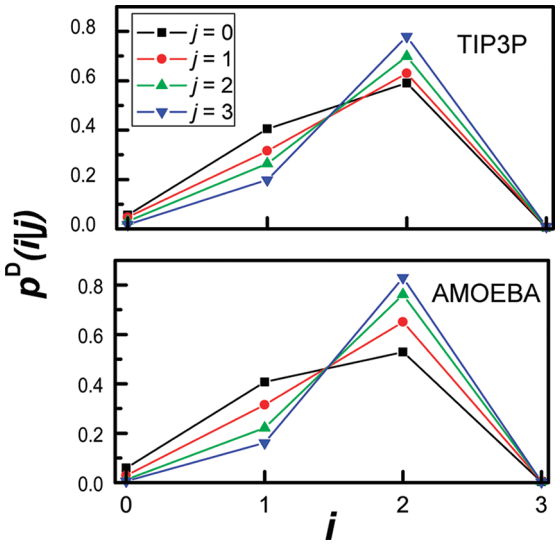

FIGURE 16. Conditional donor distributions show the probability for a water molecule to donate *i* HBs, for a fixed number *j* of acceptor HBs. Lines are drawn to guide the eye. Data at 300 K from Table 1 of ref 12.

local environment enhances the local tetrahedral structure, increasing both *i* and *j*. This agrees with earlier assessments that "spatially correlated HBs" lead to deviation from independence in the HB network.[33] Indeed, MD simulations of liquid water revealed "large rearrangements (which) involve collective motions of many water molecules",[49] its Debye relaxation was suggested to originate from collective motion of (at least) nine water molecules[10] and proton mobility requires a favorable rearrangement of two hydration shells.[11]

Anticooperative behavior is also manifested in the HB distributions of liquid water, if these indeed originate from the dissociation reaction in eq 5. The preferential dissociation of $D_2\cdots A_2$ HBs may reflect "double anticooperativity": mutual weakening of the two donor HBs in D_2 and the two acceptor HBs in A_2. Both of these correspond to unfavorable orientations: $H_2O\cdots HOH\cdots OH_2$ and $HOH\cdots O(H_2)\cdots HOH$, respectively.[45,46] Again, one is facing the dilemma that this behavior is manifested, to an extent, also in the simplest water models in which no three-body interactions were included. Hopefully, a solution may emerge from further study of explicit three-body simulation models.[46]

3. From Molecular Motions to Diffusion

Water self-diffusion is promoted by deviations from tetrahedral order, in particular through three- and five-coordinated "defects".[3−7] But how exactly do local molecular motions lead to extended translational diffusion? The microscopic picture is far from complete, perhaps because it is difficult to frame together local and collective motions. We first show that translational diffusion indeed has both characteristics and then present a quantitative application of diffusion theory to water MD, which helps elucidate some of the mechanistic details.

3.1. Local and Collective Motions. Diffusion is a random motion leading to particle excursions from its initial location to a distance *r*. If the random walk is unbiased, the particle on average goes nowhere, $\langle r\rangle = 0$. Its mean square deviation (MSD), $\langle r^2\rangle$, increases indefinitely with time *t*, with a slope proportional to the diffusion coefficient, *D*. For spherically symmetric diffusion in three dimensions, $D = \langle r^2\rangle/(6t)$. A water molecule diffusing in water is executing "self-diffusion", and its diffusion coefficient is denoted D_w. The AMOEBA simulations give $D_w = 0.23$ Å^2/ps at 300 K,[13] in excellent agreement with experiment.[37]

The AMOEBA activation enthalpy for D_w near room temperature is $E_A = 19$ kJ/mol,[13] which is also in good agreement with experiment (e.g., Figure 1 in ref 9 or Figure 2 in ref 50). This is over twice the HB strength, 8.8 kJ/mol for this model (Figure 14). Hence translational diffusion involves more extensive molecular rearrangements than cleavage of a single HB, possibly including some collective motions.

An indication for collectivity comes from comparing[9] the temperature dependence of D_w and the Debye relaxation time, τ_D, usually ascribed to collective motions.[10] If during τ_D a water molecule hops a distance *l*, its diffusion coefficient by the Einstein relation is

$$D_\tau = l^2/(6\tau_D) \tag{8}$$

Figure 17 shows very good agreement between experimental values for D_w and D_τ over a wide temperature range (extending even to amorphous solid water, see Figure 10 in ref 51). This is unexpected by the simple Debye model, in which DR is due to molecular reorientation, suggesting instead a significant translational component. Thus rotation and translation of water are coupled by its HB dynamics. MD simulations indeed suggest that a water molecule "undergoes significant displacement and reorientation when it changes its coordination number".[7]

Yet, the hopping distance thus obtained, $l = 3.29$ Å, has molecular dimensions. It coincides with the first minimum in $g(r)$ (Figure 7) and was therefore called "tetrahedral displacement".[9] Thus diffusion involves both molecular motions and larger scale correlations. What are these fundamental molecular motions? There may be different ways of looking at this question. For example, one may ask whether water self-diffusion can be decomposed into fundamental

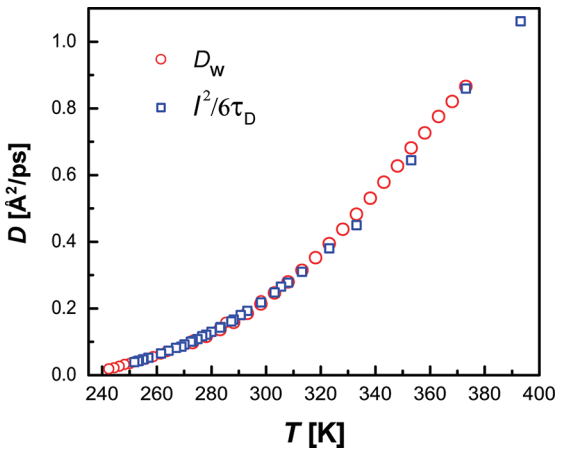

FIGURE 17. Temperature dependence of experimental data for self-diffusion and Debye relaxation time of water. Redrawn after Figure 3 of ref 9, where the sources of the data are listed.

reactions, such as "defect creating reactions", eqs 2 and 5, and "defect propagating reactions":

$$\begin{aligned} A_1 + A_2 &\rightarrow A_2 + A_1 \\ A_3 + A_2 &\rightarrow A_2 + A_3 \end{aligned} \qquad (9)$$

These identity reactions were observed to occur quite frequently in liquid water.[30] Leaving these questions for further study, we shall now consider the inverse problem of how HB dissociation can be treated by the theory of diffusion influenced reactions.[13]

3.2. Geminate Model for the Correlation Function. A frequently calculated attribute is the HB correlation function, $c(t)$, namely, the probability that two initially HBed water molecules are HBed a time t later, irrespective of their intermediate history.[13,31,52,53] This function decays nonexponentially. Previous studies suggested that the observed behavior "does not coincide with a power law decay"[31] or else is "described by a stretched exponential",[52] a manifestation of "complicated correlations between hydrogen bonds".[53] In contrast to such statements, sufficiently long trajectories for an unbound system (i.e., after "opening" the periodic simulation box) show that the long time behavior follows precisely the power-law expected from translational diffusion.

Because two specific water molecules are tracked, their kinetics can be classified as reversible geminate recombination, a problem studied intensively for excited-state proton transfer to solvent.[54,55] The simplifying assumption, which makes the equations depend on a single radial coordinate, r, is that of spherical symmetry. The relative diffusional motion of two independent particles may be replaced by a static binding site and a point particle, which diffuses with a diffusion constant $D = 2D_w$. The spherical binding site has a radius $R = 3.5$ Å, taken here as the cutoff distance in the HB definition. The bound particle may dissociate to $r = R$ (in a random direction) with a rate coefficient k_d and diffuse for $r \geq R$. Whenever it reaches $r = R$, the bound state reforms with a rate coefficient k_a. Denoting the probability density of the dissociated pair by $p(r,t)$, and the probability of the bound pair by $c(t)$, one solves the coupled equations:

$$\frac{\partial p(r,t)}{\partial t} = Dr^{-2}\frac{\partial}{\partial r}r^2\frac{\partial}{\partial r}p(r,t) + [k_d c(t) - k_a p(r,t)]\frac{\delta(r-R)}{4\pi R^2} \qquad (10a)$$

$$dc(t)/dt = k_a p(R,t) - k_d c(t) \qquad (10b)$$

Initially, $p(r,0) = 0$ and $c(0) = 1$, and the boundary condition at $r = R$ is reflective.

Luzar and Chandler[31] suggested to decouple kinetics from diffusion by simulating also $n(t)$, the probability of the pair to be unbound at $r \leq R = 3.5$ Å. Substituting it for $p(R,t)$ in eq 10b, they have adjusted k_a and k_d to obtain the best agreement between the numerically evaluated $dc(t)/dt$ and $k_a n(t) - k_d c(t)$. The additional uncertainties involved in $n(t)$ are unwarranted, because the coupled eq 10 can be solved analytically[56] or numerically with a Windows application for solving the spherically symmetric diffusion problem (SSDP, ver. 2.66).[57]

Using the same HB definition as above, we have calculated $c(t)$ from AMOEBA water simulations over an extended time regime, adjusting k_d and k_a in eq 10 to obtain a best fit.[13] The model and simulations are depicted by the dashed line and red circles in Figure 18, respectively. The agreement is very good, including in the asymptotic regime where[54]

$$c(t) \approx \frac{k_a}{k_d}\frac{1}{(4\pi Dt)^{3/2}} \qquad (11)$$

as evident from the linear behavior in the log−log scale. Thus water molecule pairs perform simple diffusive motion and HB correlations do not persist to long times.

The two rate coefficients correspond to a HB dissociation time of $k_d^{-1} = 2.6$ ps, and a bimolecular recombination rate coefficient of 1.3×10^{10} M^{-1} s^{-1}. This provides a useful procedure for eliminating "flickering events" (involving immediate HB reformation) on the HB dissociation time and a reliable method for evaluating the bimolecular recombination rate coefficient.

We have performed the calculations at different temperatures in the range 300 ± 20 K to obtain the corresponding activation energies.[13] Unlike a gas-phase reaction, where the

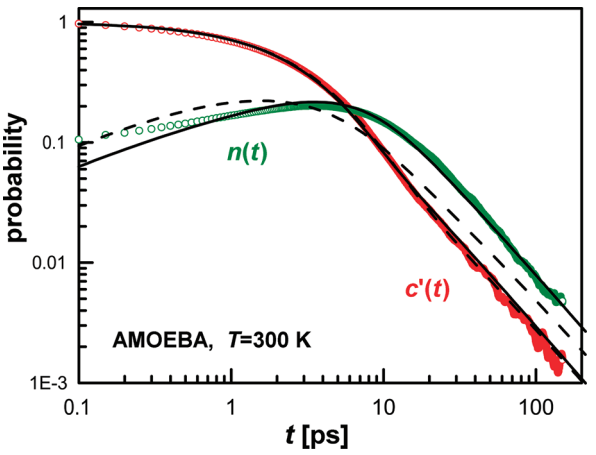

FIGURE 18. Comparison of the simulated HB correlation function, $c'(t)$ (red circles, after subtracting an initial femtosecond decay process), and of $n(t)$ (green circles) with the reversible geminate model: dashed lines, the solution of eq 10 with $k_d = 0.39$ ps^{-1} and $k_a = 21.4$ Å^3/ps; full lines, extended model, including a secondary binding site. For details, see ref 13.

activation energies for dissociation and recombination differ by the bond energy, here we find almost identical values $E_A \approx$ 16.7 kJ/mol. Hence, by the time recombination occurs the original partners have acquired new HB partners, perhaps by a series of switching reactions, so that the reactions in both directions follow a similar mechanism. Additionally, E_A is close to the value obtained above from $D(T)$ and much larger than the HB strength from the HB distribution.

We have also considered the nonbonded population, $n(t)$, as introduced in ref 31 (green circles in Figure 18).[13] Assuming that $n(t)$ equals to $p(R,t)$ times a volume factor, we find that the diffusion model predicts a maximum that occurs earlier than observed from the simulations. This could indicate that a dissociating water molecule is delayed at an interstitial site prior to diffusing away. Population in interstitial sites is observed in SDFs (e.g., Figure 6 in ref 25), and moving there may correspond to the "tetrahedral displacement" of Figure 17. The solution to eq 10 with an added secondary binding site can still be obtained analytically,[14] giving good simultaneous fits to both attributes (full lines).

4. Outlook

The plasticity of water can be traced to its asymmetric charge distribution, with a duality between tetrahedral and trigonal ligation states. This is manifested in the asymmetry of acceptor vs donor HBs, with a preponderance of OCOs over BHBs. Interestingly, just two reactions are required to convert a perfect tetrahedral arrangement into the observed HB distributions: DD/DA pair dissociation and donor switching between DAs. These distributions display cooperative and anticooperative effects even when such quantal effects were not explicitly introduced into the water model. They may stem partly from longer range correlations between HBs, which also govern the self-diffusion process. HB dissociation can be depicted by a diffusion model, suggesting some molecular events along the separation path. Despite these advances, the connection between HB defects and water dynamics is still incompletely understood.

This research was supported by The Israel Science Foundation (Grant Number 122/08). The Fritz Haber Center is supported by the Minerva Gesellschaft für die Forschung, München, FRG.

Supporting Information. A table of p_k^A and p_k^D ($k = 0-4$) from AMOEBA simulations at different temperatures. This material is available free of charge via the Internet at http://pubs.acs.org.

BIOGRAPHICAL INFORMATION

Noam Agmon received a B.Sc. in Chemistry and Physics (1974) and a Ph.D. in Theoretical Chemistry (1980) from The Hebrew University of Jerusalem and was a postdoctoral fellow in Harvard and CalTech (1981–1982). Since 1983, he has been a faculty member of the Hebrew University of Jerusalem, where he utilizes analytic theory and simulations to study proton mobility in water and proteins and diffusion influenced reactions.

FOOTNOTES

*E-mail: agmon@fh.huji.ac.il.

REFERENCES

1 Finney, J. L. Water? What's so special about it? *Philos. Trans. R. Soc. B* **2004**, *359*, 1145–1165.
2 Malenkov, G. Liquid water and ices: Understanding the structure and physical properties. *J. Phys.: Condens. Matter* **2009**, *21*, No. 283101.
3 Sciortino, F.; Geiger, A.; Stanley, H. E. Isochoric differential scattering functions in liquid water: The fifth neighbor as a network defect. *Phys. Rev. Lett.* **1990**, *65*, 3452–3455.
4 Sciortino, F.; Geiger, A.; Stanley, H. E. Effect of defects on molecular mobility in liquid water. *Nature* **1991**, *354*, 218–221.
5 Sciortino, F.; Geiger, A.; Stanley, H. E. Network defects and molecular mobility in liquid water. *J. Chem. Phys.* **1992**, *96*, 3857–3865.
6 Geiger, A.; Kleene, M.; Paschek, D.; Rehtanz, A. Mechanisms of the molecular mobility of water. *J. Mol. Liq.* **2003**, *106*, 131–146.
7 Grishina, N.; Buch, V. Dynamics of amorphous water, via migration of 3- and 5-coordinated H_2O. *Chem. Phys. Lett.* **2003**, *379*, 418–426.
8 Ball, P. Water as an active constituent in cell biology. *Chem. Rev.* **2008**, *108*, 74–108.
9 Agmon, N. Tetrahedral displacement: The molecular mechanism behind the Debye relaxation in water. *J. Phys. Chem.* **1996**, *100*, 1072–1080.
10 Arkhipov, V. I.; Agmon, N. Relation between macroscopic and microscopic dielectric relaxation times in water dynamics. *Isr. J. Chem.* **2003**, *43*, 363–371.
11 Lapid, H.; Agmon, N.; Petersen, M. K.; Voth, G. A. A bond-order analysis of the mechanism for hydrated proton mobility in liquid water. *J. Chem. Phys.* **2005**, *122*, No. 014506.
12 Markovitch, O.; Agmon, N. The distribution of acceptor and donor hydrogen-bonds in bulk liquid water. *Mol. Phys.* **2008**, *106*, 485–495.
13 Markovitch, O.; Agmon, N. Reversible geminate recombination of hydrogen-bonded water molecule pair. *J. Chem. Phys.* **2008**, *129*, No. 084505.
14 Park, S.; Agmon, N. Multi-site reversible geminate reaction. *J. Chem. Phys.* **2009**, *130*, No. 074507.

15 Gillespie, R. J.; Popelier, P. L. A. *Chemical Bonding and Molecular Geometry: From Lewis to Electron Densities*; Oxford University Press: New York, 2001.

16 Gillespie, R. J. Fifty years of the VSEPR model. *Coord. Chem. Rev.* **2008**, *252*, 1315–1327.

17 Ludwig, R. Water: From clusters to the bulk. *Angew. Chem., Int. Ed.* **2001**, *40*, 1808–1827.

18 Laing, M. No rabbit ears on water. *J. Chem. Educ.* **1987**, *64*, 124–128.

19 Buckingham, A. D. The structure and properties of a water molecule. In *Water and Aqueous Solutions*; Neilson, G. W., Enderby, J. E., Eds.; Adam Hilger: Bristol, U.K., 1986; pp 1−13.

20 Becke, A. D.; Edgecombe, K. E. A simple measure of electron localization in atomic and molecular systems. *J. Chem. Phys.* **1990**, *92*, 5397–5403.

21 Keutsch, F. N.; Saykally, R. J. Water clusters: Untangling the mysteries of the liquid, one molecule at a time. *Proc. Natl. Acad. Sci., U.S.A.* **2001**, *98*, 10533–10540.

22 Tielrooij, K. J.; Garcia-Araez, N.; Bonn, M.; Bakker, H. J. Cooperativity in ion hydration. *Science* **2010**, *328*, 1006–1009.

23 Hura, G.; Sorenson, J. M.; Glaeser, R. M.; Head-Gordon, T. A high-quality X-ray scattering experiment on liquid water at ambient conditions. *J. Chem. Phys.* **2000**, *113*, 9140–9148.

24 Korsunskii, V. I.; Naberukhin, Y. I. Does the concept of the ice-like structure of water agree with its radial distribution function? *Zh. Strukt. Khim.* **1980**, *21*, 76–81.

25 Lee, H.-S.; Tuckerman, M. E. Structure of liquid water at ambient temperature from ab initio molecular dynamics performed in the complete basis set limit. *J. Chem. Phys.* **2006**, *125*, No. 154507.

26 Paesani, F.; Iuchi, S.; Voth, G. A. Quantum effects in liquid water from an ab initio-based polarizable force field. *J. Chem. Phys.* **2007**, *127*, No. 074506.

27 Jedlovszky, P.; Brodholt, J. P.; Bruni, F.; Ricci, M. A.; Soper, A. K.; Vallauri, R. Analysis of the hydrogen-bonded structure of water from ambient to supercritical conditions. *J. Chem. Phys.* **1998**, *108*, 8528–8540.

28 Kumar, R.; Schmidt, J. R.; Skinner, J. L. Hydrogen bonding definitions and dynamics in liquid water. *J. Chem. Phys.* **2007**, *126*, No. 204107.

29 Hammerich, A. D.; Buch, V. An alternative near-neighbor definition of hydrogen bonding in water. *J. Chem. Phys.* **2008**, *128*, No. 111101.

30 Henchman, R. H.; Irudayam, S. J. Topological hydrogen-bond definition to characterize the structure and dynamics of liquid water. *J. Phys. Chem. B* **2010**, *114*, 16792–16810.

31 Luzar, A.; Chandler, D. Hydrogen-bond kinetics in liquid water. *Nature* **1996**, *379*, 55–57.

32 Jorgensen, W. L.; Chandrasekhar, J.; Madura, J. D.; Impey, R. W.; Klein, M. L. Comparison of simple potential functions for simulating liquid water. *J. Chem. Phys.* **1983**, *79*, 926–935.

33 Sciortino, F.; Fornili, S. L. Hydrogen bond cooperativity in simulated water: Time dependence analysis of pair interactions. *J. Chem. Phys.* **1989**, *90*, 2786–2792.

34 Martí, J.; Padro, J. A.; Guàrdia, E. Molecular dynamics simulation of liquid water along the coexistence curve: Hydrogen bonds and vibrational spectra. *J. Chem. Phys.* **1996**, *105*, 639–649.

35 Xu, H.; Stern, H. A.; Berne, B. J. Can water polarizability be ignored in hydrogen bond kinetics? *J. Phys. Chem. B* **2002**, *106*, 2054–2060.

36 Sutmann, G.; Vallauri, R. Dynamics of the hydrogen bond network in liquid water. *J. Mol. Liq.* **2002**, *98−99*, 213–224.

37 Ren, P.; Ponder, J. W. Temperature and pressure dependence of the AMOEBA water model. *J. Phys. Chem. B* **2004**, *108*, 13427–13437.

38 Giguère, P. A. The bifurcated hydrogen-bond model of water and amorphous ice. *J. Chem. Phys.* **1987**, *87*, 4835–4839.

39 Newton, M. D. Small water clusters as theoretical models for structural and kinetic properties of ice. *J. Phys. Chem.* **1983**, *87*, 4288–4292.

40 Bergman, D. L. Topological properties of the hydrogen-bond network in liquid water. *Chem. Phys.* **2000**, *253*, 267–282.

41 Rozas, I.; Alkorta, I.; Elguero, J. Bifurcated hydrogen bonds: Three-centered interactions. *J. Phys. Chem. A* **1998**, *102*, 9925–9932.

42 Kaatze, U.; Behrends, R.; Pottel, R. Hydrogen network fluctuations and dielectric spectrometry of liquids. *J. Non-Cryst. Solids* **2002**, *305*, 19–28.

43 Laage, D.; Hynes, J. T. A molecular jump mechanism of water reorientation. *Science* **2006**, *311*, 832–835.

44 Reed, A. E.; Curtiss, L. A.; Weinhold, F. Intermolecular interactions from a natural bond orbital, donor-acceptor viewpoint. *Chem. Rev.* **1988**, *88*, 899–926.

45 Ojamäe, L.; Hermansson, K. Ab initio study of cooperativity in water chains: Binding energies and anharmonic frequencies. *J. Phys. Chem.* **1994**, *98*, 4271–4282.

46 Tainter, C. J.; Pieniazek, P. A.; Lin, Y.-S.; Skinner, J. L. Robust three-body water simulation model. *J. Chem. Phys.* **2011**, *134*, No. 184501.

47 Lenz, A.; Ojamäe, L. Theoretical IR spectra for water clusters $(H_2O)_n$ (n = 6−22, 28, 30) and identification of spectral contributions from different H-bond conformations in gaseous and liquid water. *J. Phys. Chem. A* **2006**, *110*, 13388–13393.

48 Kühne, T. D.; Pascal, T. A.; Kaxiras, E.; Jung, Y. New insights into the structure of the vapor/water interface from large-scale first-principles simulations. *J. Phys. Chem. Lett.* **2011**, *2*, 105–113.

49 Ohmine, I. Liquid water dynamics: Collective motions, fluctuations, and relaxation. *J. Phys. Chem.* **1995**, *99*, 6767–6776.

50 Price, W. S.; Ide, H.; Arata, Y. Self-diffusion of supercooled water to 238 K using PGSE NMR diffusion measurements. *J. Phys. Chem. A* **1999**, *103*, 448–450.

51 Smith, R. S.; Dohnálek, Z.; Kimmel, G. A.; Stevenson, K. P.; Kay, B. D. The self-diffusivity of amorphous solid water near 150 K. *Chem. Phys.* **2000**, *258*, 291–305.

52 Starr, F. W.; Nielsen, J. K.; Stanley, H. E. Hydrogen-bond dynamics for the extended simple point-charge model of water. *Phys. Rev. E* **2000**, *62*, 579–587.

53 Lee, H.-S.; Tuckerman, M. E. Dynamical properties of liquid water from ab initio molecular dynamics performed in the complete basis set limit. *J. Chem. Phys.* **2007**, *126*, No. 164501.

54 Agmon, N.; Pines, E.; Huppert, D. Geminate recombination in proton-transfer reactions. II. Comparison of diffusional and kinetic schemes. *J. Chem. Phys.* **1988**, *88*, 5631–5638.

55 Agmon, N. Elementary steps in excited-state proton transfer. *J. Phys. Chem. A* **2005**, *109*, 13–35.

56 Kim, H.; Shin, K. J. Exact solution of the reversible diffusion-influenced reaction for an isolated pair in three dimensions. *Phys. Rev. Lett.* **1999**, *82*, 1578–1581.

57 Krissinel', E. B.; Agmon, N. Spherical symmetric diffusion problem. *J. Comput. Chem.* **1996**, *17*, 1085–1098.